Article)

Fate of ZnS:Mn quantum dots in Seine River water and sea-water. Ecotoxicological effects on Chlorella Vulgaris microalgae.

Bingbing Deng [1,4]*, Rania Maaloul [1], Sophie Nowak [1], Yann Sivry [2], Claude Yéprémian [3], Souad Ammar [1], Fayna Mammeri [1]*, and Roberta Brayner [1]†

[1] Université Paris Cité, CNRS, ITODYS, F-75013 Paris, France; dengbingbcugb@163.com (B.D.), rania.maaloul@universite-paris-saclay.fr (R.M.), sophie.nowak@u-paris.fr (S.N.), ammarmer@univ-paris-diderot.fr (S.A.), fayna.mammeri@u-paris.fr (F.M.)
[2] Université Paris Cité, CNRS, IPGP, F-75005 Paris, France; yann.sivry@u-paris.fr
[3] CNRS, Museum Natl Hist Nat, Mol Commun & Adaptat Microorganismes MCAM, UMR 7245, CP 39,57 Rue Cuvier, F-75005 Paris, France
[4] Advanced Materials Division, Suzhou Institute of Nano-Tech and Nano-Bionics, Chinese Academy of Sciences, Suzhou, 215123, China
† *In memoriam*
* Correspondence: fayna.mammeri@u-paris.fr (F.M.); dengbingbcugb@163.com (B.D.)

Abstract:

The release of engineered materials into the environment can have detrimental effects on living organisms in ground, rivers, and oceans. Despite the increasing use of nanomaterials, little research is conducted on their degradation. Understanding the biology and environmental consequences of manufactured materials is crucial for preserving the environment and developing more respectful chemistry protocols. Physicochemical studies are essential to understand material behavior and their uptake and distribution within microorganisms. II-VI semiconducting nanocrystals, like ZnS nanoparticles, have emerged due to their quantum confinement, allowing for customization of electronic and optical properties. To assess the toxicity of ZnS QDs doped with Mn^{2+} and perform ecotoxicological tests, a suitable natural environment and an aquatic model are needed. Microalgae, like Chlorella Vulgaris, offer advantages in ecotoxicology, including environmental relevance, sensitivity, experimental feasibility, ethical considerations, and comparative studies. This paper presents the synthesis of ZnS:Mn NPs with varying concentrations of Mn^{2+}. These NPs induce an antioxidant defense system in algal cells, which may be toxic to Chlorella vulgaris via an oxidative stress mechanism. The toxicity of manganese-doped ZnS nanoparticles does exist but is lower than that induced by a Mn^{2+} ion concentration of 100 mg L^{-1}.

Keywords: nanoparticles; toxicological impact; toxicity; quantum dots; behavior; dissolution, risk, fate.

1. Introduction

The release of engineered materials into the environment may have a detrimental effect on living organisms in the ground, the rivers, and the oceans. Despite the increasing use of nanomaterials in various devices, very little research is conducted on the degradation of manufactured materials while many studies have focused on the impact of these materials on plants and their possible entry into the food chain. As many people are afraid of nanotechnologies, the interest in understanding the biology and environmental consequences of manufactured materials is increasing [1,2]. A better understanding of toxicological mechanisms will not only make it possible to better preserve the environment but also to practice better chemistry, through the development of protocols that are more

respectful of nature. For that, physicochemical studies are essential to understand the behaviour of the materials, as well as their uptake and distribution inside microorganisms [3–7]. For an environmental risk assessment of nanoparticles, both exposure in the environment (dissolution/aggregation) and hazards, such as toxicity, need to be considered.

Among all the manufactured nanomaterials, II-VI semiconducting nanocrystals emerged due to their quantum confinement, providing to tailor the electronic and optical properties by tuning the size of the particles [8,9]. ZnS nanoparticles are sought for several applications such as displays [10]. Various colours can be obtained by doping the particles [11–16] since the dopants are acting as emitting centres within the quantum-confined crystalline structure of the QDs [17,18]. To produce an orange wavelength (580-590 nm), manganese is one of the most common dopants in ZnS: as a divalent cation, Mn^{2+} can substitute zinc in the blende lattice. The emission peak is generally ascribed to the electronic transition between $^4T_1$ and $^6A_1$ energy levels of tetrahedral $[MnS_4]^{6-}$ molecular species [12]. However, as the potential of ZnS nanoparticles continues to be explored, so does the need for understanding their environmental impact and potential toxicity.

To assess the toxicity of such ZnS QDs doped with Mn^{2+} and perform ecotoxicological tests, it is necessary to find a suitable natural environment and an aquatic model. Microalgae represent excellent aquatic models since they can breed in lakes and seas, which are rich enough in nutrients to cultivate microalgae. Seine river water is very rich in mineral salts [19–22] for cultivating microorganisms. Microalgae are used for the treatment of wastewater [23,24] and have been proven to efficiently assimilate nutrients from wastewater. Moreover, they are easy to cultivate, present a quite short growth period (< 1 week), and are responsive to pollutants. Such algal species have been found to exhibit interesting capabilities for the removal of several environmental pollutants. Chlorella Vulgaris, a widely studied model microalga, has become an indispensable organism in ecotoxicology due to its sensitivity and pivotal role as a primary producer in aquatic ecosystems. This microalga plays a significant role in the food chain, influencing the health of diverse aquatic organisms. Studying the toxicity of ZnS nanoparticles using Chlorella Vulgaris offers several advantages such as environmental relevance (Chlorella Vulgaris is a common microalga found in various aquatic environments), sensitivity and responsiveness (highly sensitive to environmental changes, including exposure to various pollutants, ca. 72-96 hours, making it an excellent bioindicator for assessing the toxic effects of ZnS NPs [25–27]), experimental feasibility (Chlorella Vulgaris is easy to cultivate and maintain in laboratory settings. These microalgae can be cultured in large quantities under controlled conditions, ensuring reproducibility and facilitating toxicological studies with minimal logistical challenges), ethical considerations, and comparative studies (due to the widespread use of Chlorella Vulgaris as a model organism, toxicity data obtained using this microalga can be compared across different studies, institutions, and countries).

In this paper, we intend to assess the toxicity of ZnS:Mn nanoparticles (synthesized by the polyol process) in the presence of Chlorella Vulgaris in either Seine River water or synthetic seawater. Indeed, Mn^{2+} can be dissolved in the water system, which could be toxic to Chlorella vulgaris, after the dissolved Mn^{2+} or the ZnS:Mn NPs go inside the algal cells and influence the activity of chloroplast and mitochondria, by inducing the ROS (reactive oxygen species), and then leading to the cell death.

2. Materials and Methods

2.1. Synthesis of Mn-doped ZnS quantum dots by polyol method

All chemicals are of analytical grade and were used without any further purification. Manganese acetate tetrahydrate (≥ 99%, $Mn(CH_3COO)_2.4H_2O$), trioctylphosphine oxide (TOPO, $(CH_3(CH_2)_7)_3PO$), diethylene glycol (DEG) ($OH(CH_2)_2O(CH_2)_2OH$) purchased

from Sigma-Aldrich, thiourea (99%, $SC(NH_2)_2$) purchased from Alfa Aesar, and zinc acetate dihydrate (98+%, $Zn(CH_3COO)_2.2H_2O$) purchased from Acros Organics.

Zinc acetate dihydrate ($Zn(CH_3COO)_2.2H_2O$, 87.8 mg) and manganese acetate tetrahydrate ($Mn(CH_3COO)_2.4H_2O$, 1.0 mg, 4.1 mg, 8.5 mg and 24.5 mg) were mixed in a three-neck flask with 80 mL of diethylene glycol (DEG) to synthesis ZnS: Mn (0.5%), ZnS: Mn (2.0%), ZnS: Mn (4.0%), ZnS: Mn (10%), respectively, in presence of thiourea (38.8 mg) and TOPO (193.3 mg). All the reagents were dissolved in DEG with 20 min of sonication, then the solutions were heated to 180 °C for 30 min; after that, ZnS: Mn (0.5%), ZnS: Mn (2.0%), ZnS: Mn (4.0%), ZnS: Mn (10%) NPs were recovered after 3 cycles of centrifugation (at 22 000 rpm) and washing with ethanol, then dried at 60 °C overnight.

2.2 Characterization of ZnS:Mn QDs

X-Ray Diffraction (XRD) patterns of the nanoparticles (NPs) have been recorded on an X'Pert Pro Pananalytical diffractometer, using the Co Kα radiation, in the range 10-80° (2θ) with a scan step of 0.016°. The peak indexing was performed using the Highscore Plus software and the Database ICSD-Panalytical. The cell parameter and the size of the coherent diffraction domain were determined with MAUD software [28], based on the Rietveld method.

The surface chemical composition of the NPs has been checked by X-ray Photoelectron Spectroscopy (XPS) using a Thermo VG ESCALAB 250 instrument equipped with a micro-focused monochromatic Al Kα X-ray source (1486.6 eV) and a magnetic lens. The X-ray spot size was 500 μm (15 kV, 150 W). The spectra were acquired in the constant analyzer energy mode with a pass energy of 100 and 40 eV for the survey spectra and the narrow high-resolution regions, respectively. The "Avantage" software (version 4.67) was used for data acquisition and processing. The C1s peak at 285 eV, due to the adventitious contamination, was used as a reference to calibrate the binding energies for charge correction.

Cations / S ratios were carried out by X-ray fluorescence spectrometry (XRF). Nanopowders were dispersed in demineralized water, and then 20 μl were taken, deposited on a clean polycarbonate membrane, and dried. Finally, the membranes were analyzed on an Epsilon 3XL (Panalytical) XRF spectrometer equipped with a silver X-ray tube operating at different conditions: 20kV and 15μA current emissions for Mn, 50 kV and 6μA for Zn, 10 kV and 30 μA for S. A certified solution of Mn, Zn, and S (Inorganic Ventures 1 g L^{-1}) was used for calibration in perfectly identical conditions, in the range 0 to 30 μg.

The morphology of the NPs has been determined by Transmission Electron Microscopy (TEM), using a JEOL-100 CX II microscope operating at 100 kV. The mean diameter and standard deviation were inferred from image analysis of ca. 250 particles using ImageJ software.

Dynamic Light Scattering (DLS) and zetametry were performed using Zetasizer from Malvern to determine the size distribution and the surface charge of the NPs; their ζ potential was measured at room temperature starting from their aqueous solution (1 g L^{-1}), after vigorous sonication for 10 min.

The concentration of Mn and Zn were determined using ICP-AES (ICAP 6200 Thermo Fisher, Thermo Fisher Scientific, Waltham, MA, USA). Detection and quantification limits were 0.20 ppb and 0.67 ppb respectively, for Zn and of 0.02 ppb and 0.07 ppb respectively, for Mn. The standard deviation associated with the measurements was smaller than 5%.

2.3. Chlorella vulgaris culture

Chlorella vulgaris were provided by the Museum National d'Histoire Naturelle (MNHN) Culture Collection. Chlorella vulgaris is a planktonic eukaryotic single-cell green algae, which was cultivated in the 75 cm^2 cell culture flask bought from Thermofisher in (i) sterile BG11 medium (pH 7.30), (ii) Seine River water (SRW, pH 8.11) and (iii) synthetic seawater (SSW, pH 7.81) (Supplement information 1). Took 15 ml chlorella

vulgaris collection culture and mixed with 45 ml of different media, then all the cultures were kept at a controlled temperature of 25 °C and a daily cycle of 16 h of luminosity (50-80 μmol m^2 s^1 photosynthetic photon flux, PPF) under ambient CO_2 environment.

2.4. Toxicity assessments

Viability test has been done using the Cellometer Auto T4 manufactured by Nexcelom.

SOD (Superoxide dismutase) enzymatic activity measurements were performed using 19,160 SOD determination kit from Sigma-Aldrich (France). SOD enzymatic activity was determined using colorimetric measurements by a kinetic method and then read at 450 nm using an Envision Multilabel Plate Reader (Perkin-Elmer, USA).

Adenosine-5′-triphosphate (ATP) level of the samples were detected using the luciferase-luciferin enzymatic assay kit BacTiter-Glo™ ordered from Progema (France). The ATP can be released from algae cell easily with the cell lysis in this kit, and we do not need to wash cells or remove the medium, the reagent can be added to the microplate well directly. The plate reader will be used to quantitative determinate the ATP, and the relative luminescent units were detected with an Envision Multilabel Plate Reader equipped with a luminescent optical filter. All experiments were done in triplicate.

Biomass transmission electron microscopy (TEM) studies was performed with a Hitachi H-700 (Tokyo, Japan) operating at 80 kV equipped with a Hamatsu camera. The microalgae were first fixed with a mixture containing 2% glutaraldehyde and picric acid in a phosphate Sorengën buffer (0.1 M, pH 7.4). Cells were contrasted with 0.5% of osmium tetraoxyde. Dehydration was then achieved in a series of ethanol baths, and the samples were processed for flat embedding in a Supper resin, then ultrathin sections of samples in the resin were made using a Reicherd E Young Ultracut ultramicrotome (Leica, Wetzlar, Germany).

3. Results and Discussion

3.1. Structural characterization of ZnS:Mn NPs

The X-ray diffraction patterns of these NPs are presented in Figure 1. The diffraction peaks of these samples, at 33°, 56°, 67°, are matching well with the (111), (220), (311) crystalline planes of cubic ZnS phase (COD no. 5000088). No other impurity phase was found, evidencing the high purity of the ZnS:Mn NPs, even small in size. The broadness of the peaks is evidencing the nanocrystalline size of the samples [29]. The crystal size of each sample has been calculated through computational Rietveld refinements using MAUD software (Materials Analysis Using Diffraction), which was ranging from 1.1 to 1.5 nm. The average crystalline size of these ZnS NPs was also estimated using the diffraction peaks full width at half maximum (FWHM) by Debye-Scherrer's formula [29,30]:

$$D = \frac{k\lambda}{\beta cos\theta}$$

where D is the average size of the particles, k is the particles shape factor (0.89), λ is the X-ray wavelength (0.17889 nm), β is the FWHM of the diffraction peak, θ is the diffraction Bragg angle. The calculation average crystalline sizes of ZnS:Mn (0.5%, 2.0%, 4.0% and 10%) NPs ranged from 2.3 nm to 2.5 nm, which agrees with the average diameter deduced from TEM analysis (2.3 ± 0.5 nm) (Figure 4). The Debye-Scherrer's formula calculated size and the TEM statistical size are a little bigger than the actual crystal size due to the 2θ, measurement boundary and other factors.

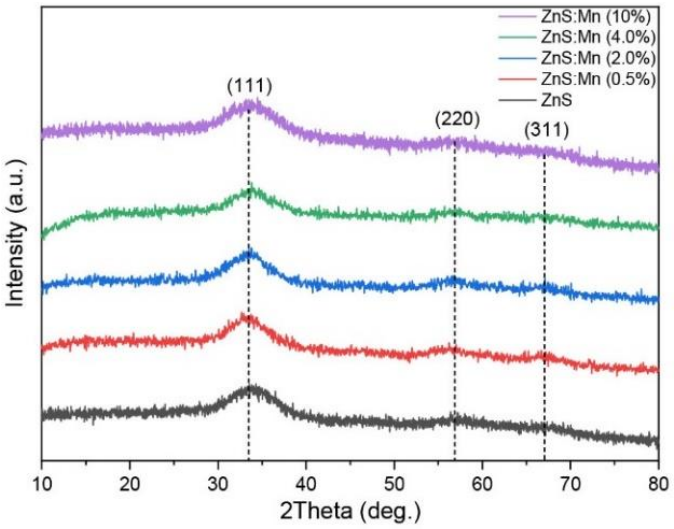

Figure 1. XRD patterns of all the produced ZnS: Mn NPs.

Table 1 gathers the elemental compositions of ZnS:Mn nanoparticles deduced from XRF analysis: the Mn content in the NPs increased while increasing the Mn molar concentration, although it does not match well with the expected Mn molar concentration. One can notice that sulphur is a volatile element that is often very difficult to calibrate and measure; this can explain the observed deviations from what is expected.

Table 1. Elemental composition XRF of all the produced ZnS: Mn NPs, deduced by XRF.

NPs		Zn	S	Mn	$Mn/(Mn+Zn)_{exp}$	$Mn/(Mn+Zn)_{XRF}$
ZnS: Mn (0.5%)	mass (µg)	32.315	11.034	0.048		
	%mol	58.9	41.0	0.10	0.005	0.002
ZnS: Mn (2.0%)	mass (µg)	46.842	14.838	0.668		
	%mol	60.1	38.8	1.1	0.020	0.018
ZnS: Mn (4.0%)	mass (µg)	22.464	8.427	0.427		
	%mol	55.9	42.8	1.3	0.040	0.023
ZnS: Mn (10%)	mass (µg)	8.336	3.5	1.420		
	%mol	48.6	41.6	9.8	0.100	0.168

The surface chemical composition of these NPs was investigated by XPS analysis [31]. The survey spectra of ZnS: Mn (0.5%, 2.0%, 4.0% and 10%) NPs are presented in Figure 2; the binding energy of Zn $2p_{1/2}$ and Zn $2p_{3/2}$ are centered at 1045.8 eV and 1022.9 eV, respectively, which confirm that Zn atom exists only in the form of Zn^{2+}, whereas the S 2p peak at 161.4 eV is characteristic of S^{2-} species [32,33]. The XPS semi-quantitative data gave atomic Zn/S ratio of 1:0.9; 1:1; 1:1 and 1:0.9, for the samples 0.5%, 2.0%, 4.0% and 10% respectively, that lies reasonably close to the ideal 1:1 ratio for every sample. Peaks corresponding to C and O adventitious contaminations were also observed in all spectra. The slight error on the Zn/S ratio (equal to 0.9) may raise suspicion of oxidation of the nanoparticles. However, the O 1s peak observed at 532.0 eV cannot be attributed to O atoms belonging to a ZnO crystalline system, since the signal originated from ZnO would appear at 530 eV. Hence, the O 1s peak at 532 eV may be assigned to chemisorbed oxygen species [32].

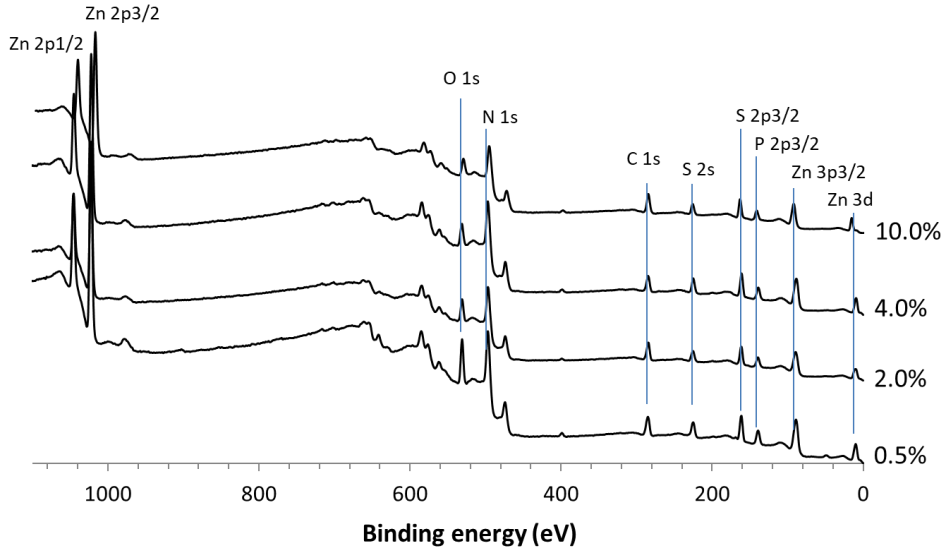

Figure 2. XPS survey spectra of ZnS: Mn (0.5%, 2.0%, 4.0% and 10%) NPs, the spectra were calibrated by setting the main C 1s at 285 eV.

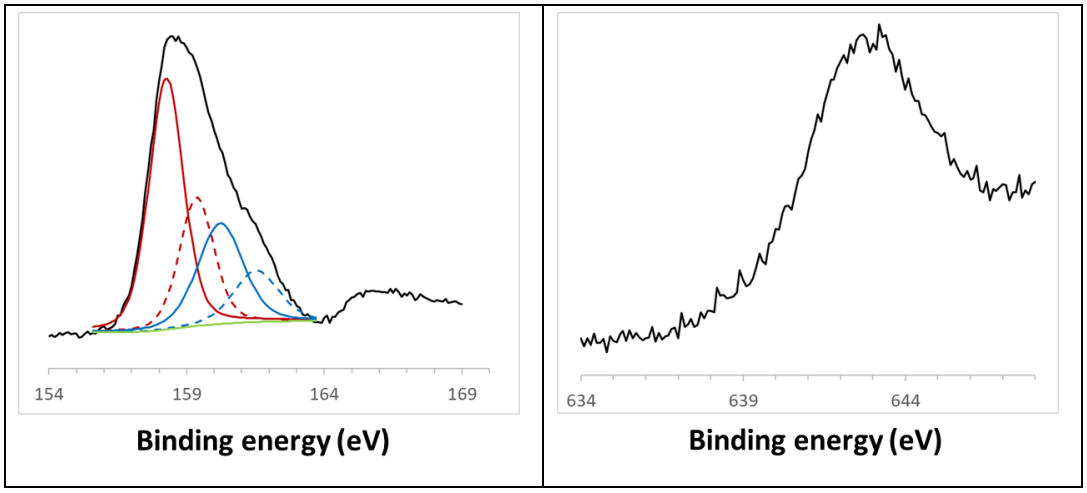

Figure 3. High resolution spectra of S 2p, and Mn 2p signals recorded on ZnS: Mn NPs with 10% Mn.

The high-resolution spectra of S 2p and Mn 2p elements are shown in Figure 3. The intensity ratio of the spin–orbit splitting peaks for S $2p_{3/2}$ and S $2p_{1/2}$ was approximately 2:1, in good agreement with the presence of Zn^{2+} linked only to S atoms [34]. The S 2p asymmetric spectra may be fitted with two components for ZnS:Mn (10%) NPs, each fitted with two peaks, corresponding to S $2p_{3/2}$ and S $2p_{1/2}$. The binding energy of 158-159 eV originated from S^{2-} in the ZnS structure while the subpeak at approximately 160-161 eV may be due to surface defects of the S–S species in the ZnS shell layer as it was previously reported for ZnS nanorods [35]. One can notice, on these two spectra, a lower intensity S 2p peak at 167.9 eV, attributed to the oxidized SO_4^{2-} form [36,37], due to a very slight and negligible oxidization of the surface of ZnS:Mn NPs. The spectra were less and less noisy as the Mn content increases [38–40] while the Mn $2p_{3/2}$ peak was centered at around 642 eV, corresponding to Mn^{2+} [41]. The XPS semi-quantitative data gave atomic Mn/S ratio of 0.02:1; 0.03:1; 0.04:1; 0.08:1, for the samples 0.5%, 2.0%, 4.0% and 10% respectively, that lies reasonably close to the ideal ratio for every sample.

Transmission electron microscopy (TEM) images of different molar concentration of Mn doped ZnS NPs are shown in Figure 4 and Figure S1. The TEM pictures gave lattice information and confirmed the blende structure of the crystallized ZnS:Mn (0.5%, 2.0%, 4.0%, and 10%). The statistical analysis of the size distribution of these NPs indicated an average size of ca. 2.3 ± 0.5 nm. In addition, EDX analysis showed that all these NPs mainly contain Mn, Zn and S elements, Cu being a constitutive element of the grid and Cr coming from the TEM machine; hence, we can assume that no impurity was found in these ZnS:Mn NPs.

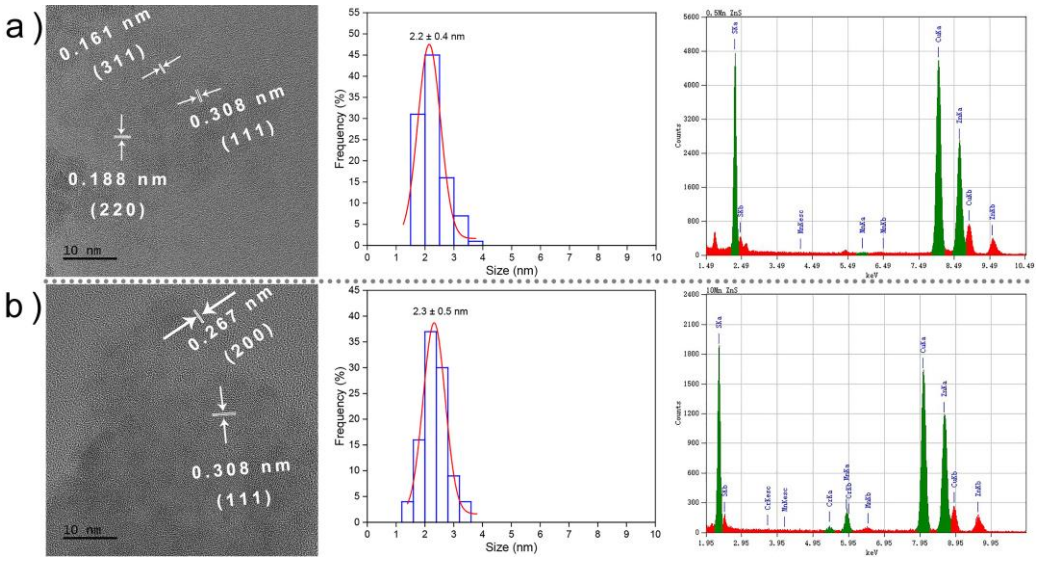

Figure 4. TEM image, size distribution and EDS of a) 0.5% ZnS: Mn and b) 10% ZnS: Mn. (2.0% and 4.0% Mn doped ZnS are shown in Figure S1).

The size and colloidal stability of the NPs were determined by dynamic light scattering (DLS), in 3 different types of water, at various pH (Figure 5 and Figure S2). Whatever the medium and the pH, the nanoparticles were aggregated, but to a different degree. In a BG11 water (or fresh water), at pH = 2, all the NPs formed what will be called small aggregates since the size of the colloids was around 340 nm for ZnS:Mn (0.5%) and ZnS:Mn (4.0%) NPs, and 460 nm and 400 nm for ZnS:Mn (2.0 %) and ZnS:Mn (10 %) respectively. However, in a more basic medium (pH = 8), the size of almost all the colloids was greater than 1000 nm, only that of ZnS:Mn (4.0%) remained less than 340 nm. In the Seine River water, all the colloids were more stable, with sizes between 340 nm and 530 nm at dif-

ferent pH, except the ZnS: Mn (4.0%) NPs which formed aggregates of 220 nm at pH 4 and larger than 2000 nm at pH 10. Moreover, the size of these colloids was smaller in seawater, in an acid medium (less than 400 nm at pH 6), and it could exceed 1000 nm at pH 10. Above all, we could conclude that the size of these NP aggregates was more stable in BG11 and in seawater in an acidic environment. Colloids were stable (300 to 500 nm) in Seine River water, whether the medium is acidic or alkaline, except for ZnS:Mn (4.0%) NPs, which were unfortunately easier to aggregate when the pH varied from 6 to 8. Indeed, one should know that the pH of culture of Chlorella vulgaris in the different water systems varies from 7.4 to 8.7.

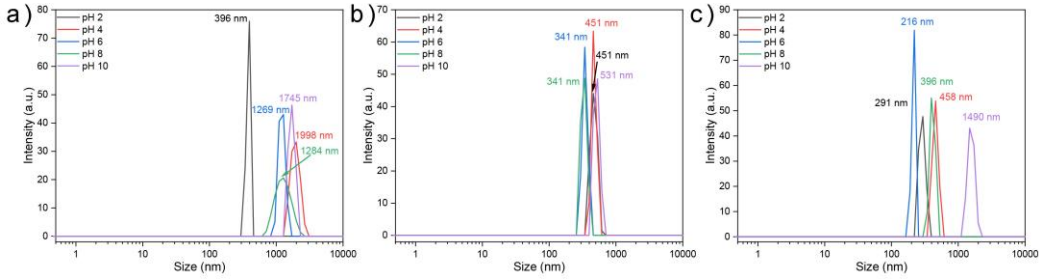

Figure 5. Size of ZnS: Mn (10%) NPs in (a) BG11, (b) Seine River water, (c) Synthetic seawater. (0.5%, 2.0% and 4.0% Mn doped ZnS NPs are shown in Figure S2).

Figure 6 and Figure S3 present the zeta potential measurements performed on all the NPs produced, in the three different water systems at different pH. We observed that the NPs were relatively stable in an alkaline medium either in BG11 and Seine River water, whereas they were likely unstable in synthetic seawater, whatever the pH, not only alkaline but also acid. We also observed that these NPs were negatively charged when the pH varied from 6 to 8, which means that the NPs may be not easy to internalize by the algae cell (the zeta potential of the algae cell is about -8.82 eV) due to repulsive electrostatic interactions with the cell membrane [42,43].

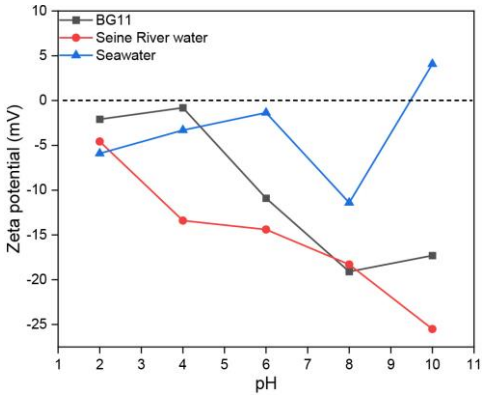

Figure 6. Zeta potential of ZnS: Mn (10%) NPs in different water systems. (0.5%, 2.0% and 4.0% Mn doped ZnS NPs are shown in Figure S3).

Although nanoparticles tend to aggregate in water, whatever the pH, they can be dissolved. Therefore, we followed the dissolution of ZnS:Mn (10%) by ICP-AES. Figure 7 presents the concentration of Mn^{2+} and Zn^{2+} in the 3 different water systems after dissolving the ZnS:Mn (10%) NPs. The dissolution of Mn^{2+} was generally higher in synthetic seawater and in Seine River water than in Milli-Q water. Moreover, in Milli-Q water, the dissolution of Mn^{2+} was maximum on the 2nd day, whereas it reached a maximum on the 4th or 5th day in seawater and in Seine River water. Surprisingly, the dissolution of Zn^{2+}

was totally different: in seawater, the concentration of dissolved Zn^{2+} remained stable for a week, which is probably due to a saturation of seawater with Zn^{2+} ions; however, in the Seine River water and Milli-Q water, the dissolution of Zn^{2+} continued and increased over time.

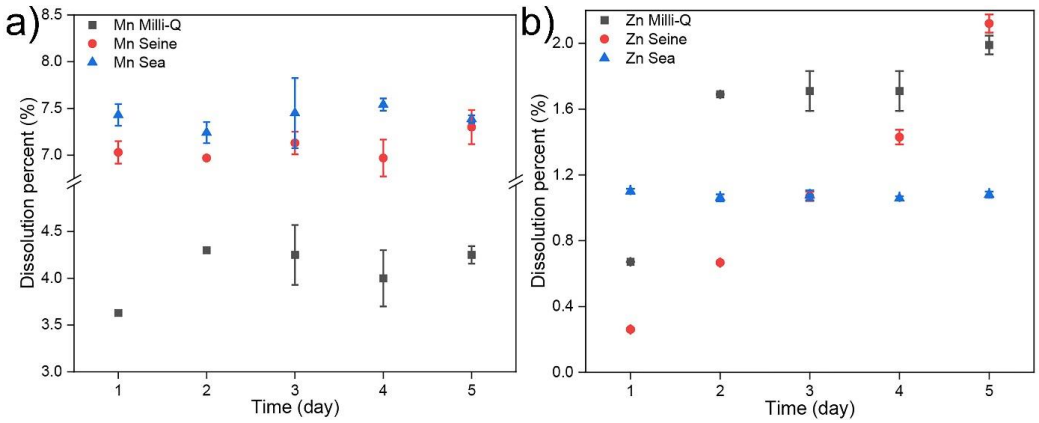

Figure 7. Dissolution of ZnS: Mn (10%) NPs in different water systems: monitoring of a) Mn^{2+} and b) Zn^{2+} concentrations in different water systems.

3.2. Assessment of the toxicity of ZnS:Mn nanoparticles

The specific toxicity of nanoparticles for Chlorella Vulgaris may vary depending on several factors, including composition, nanoparticle size, concentration, surface coating, exposure duration, etc. Zns:Mn NPs, as other nanomaterials, have the potential to interact with living organisms differently from their bulk counterparts due to their unique properties at the nanoscale. When Chlorella vulgaris is exposed to nanoparticles, various biological processes, such as cellular uptake, oxidative stress, or changes in biochemical pathways, can be affected. The resulting effects may include inhibited growth, reduced photosynthesis, lower cell viability, and altered metabolic activities. To the best of our knowledge, there have been limited studies specifically examining the toxicity of ZnS nanoparticles doped with manganese on Chlorella vulgaris.

The hazard statements of the starting reagents to conduct the synthesis of ZnS:Mn NPs by the polyol process are presented in Table 2. The toxicity of thiourea comes essentially from its ability to react through the -SH group or to release cyanide (CN^-) ions upon metabolism while that of Zn acetate comes from the Zn^{2+} ions released in solution, since Zn is a heavy metal.

In order to investigate whether the toxicity came from Mn^{2+} ions or from the NPs themselves, $Mn(CH_3COO)_2.4H_2O$ salt, pure ZnS NPs and ZnS:Mn NPs were added successively into the three different culture media of Chlorella vulgaris: BG11, Seine River water (SRW), and synthetic seawater (SSW). One week later, the different concentrations of NPs (20 mg L^{-1}, 50 mg L^{-1}, and 100 mg L^{-1}) were added into the three types of aqueous medium; each medium repeated in 4 culture flasks (three research groups and a control group). Relative toxicity measurements such as cell viability, superoxide dismutase (SOD) activity and mitochondria activity were performed over the next 5 continuous days after exploring in the NPs environment. Then, we could evaluate the toxic effect of NPs by comparing with the control group.

Table 2. Hazard statements of the reagents used for the synthesis of ZnS: Mn NPs (ref From VWR website, Accessed on the purchasers' websites on 28th July 2023.).

Common name	Hazard statements
Trioctylphosphine oxide (TOPO, $(CH_3(CH_2)_7)_3PO$), Sigma-Aldrich	
Manganese acetate tetrahydrate ($\geq$ 99%, $Mn(CH_3COO)_2.4H_2O$), Sigma-Aldrich	
Diethylene glycol (DEG) ($OH(CH_2)_2O(CH_2)_2OH$), Sigma-Aldrich	
Thiourea (99%, $SC(NH_2)_2$), Alfa-Aesar	
Zinc acetate dihydrate (98+%, $Zn(CH_3COO)_2.2H_2O$), Acros Organics	

3.2.1. Toxicity of ZnS NPs

Figure 8 presents the viability of Chlorella vulgaris in different aqueous media, in contact with ZnS NPs. In BG11 and SSW media, viability decreased immediately, from the first day of testing until the last day compared to the control group. Viability recovers 48 h later in the presence of lower concentrations of NPs (20 mg L^{-1} and 50 mg L^{-1}). In Seine River water, the viability decreased throughout the first days of the test in the presence of high concentrations of NPs (50 mg $L^{-1}$and 100 mg L^{-1}) except on the 4th day of the test. Algae showed much lower viability (less than 40%) in SRW and SSW media; it could be assumed either that the culture media influenced the expression of cell membrane proteins [44,45] or that the ZnS NPs were very strongly aggregated on the surface of the algae, and thus disturbed the transport function of the cellular membrane. This led to a decrease in the availability of nutrients necessary for algae growth [44]. Therefore, we can conclude that ZnS NPs presents a relatively weak toxic effect on Chlorella vulgaris, in agreement with previous work [46,47]. Not surprisingly, high concentrations of NPs were more toxic than lower concentrations.

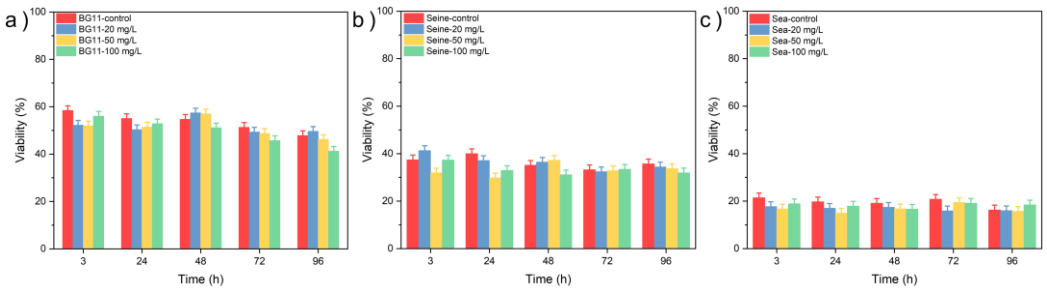

Figure 8. Viability tests of Chlorella vulgaris in a) BG11, b) SRW, c) SSW culture media contacted with pure ZnS NPs.

3.2.2. Toxicity of Mn^{2+}

The toxicity of Mn^{2+} was also addressed, by introducing solutions of Mn^{2+} at the concentrations of 20 mg L^{-1}, 50 mg L^{-1}, and 100 mg L^{-1}. Figure 9 shows Chlorella vulgaris in the presence of Mn^{2+} ions 96 hours after their introduction. We observed that the color of the cultures carried out in Seine River Water and synthetic seawater and containing Mn^{2+} ions was deeper than that of the control groups. The Seine River water was even darker…

Figure 9. Chlorella vulgaris in the different culture medium.

Figure 10 shows the viability of Chlorella vulgaris: in BG11 water, the viability remained almost stable in the presence of Mn^{2+} concentrations below 100 mg L^{-1}; when the concentration of Mn^{2+} was 100 mg L^{-1}, the viability decreased drastically during the first four days of the test. In Seine and sea waters, viability decreased in a variable way: it is probably caused by a paucity of nutrients, such as nitrates, phosphates or carbon sources (for example glucose), absent in Seine and sea waters [44,48]. Consequently, the physiological state of the algae became very bad due to the lack of nutrients [44]. Then, they showed less resistance to the bad water environment or even toxic Mn^{2+} ions. In BG11, the algae had all the adequate nutrients, which led to a completely different behavior. Consequently, a high concentration of Mn^{2+} ions (for example, 100 mg L^{-1}) was highly toxic for Chlorella vulgaris in all culture media, but even more particularly in SSW medium.

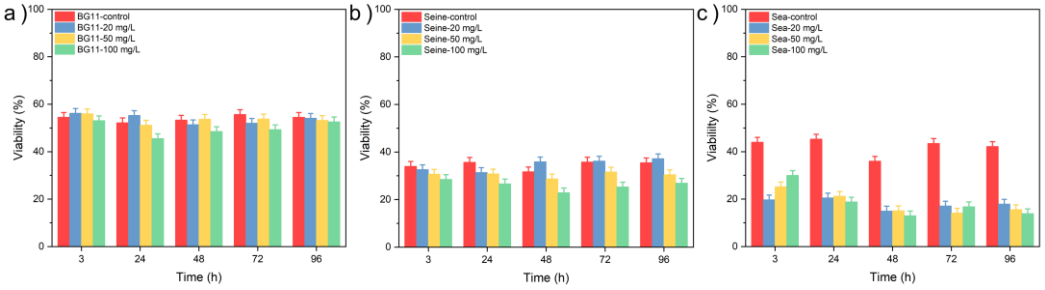

Figure 10. Viability tests of Chlorella vulgaris in a) BG11, b) SRW, c) SSW culture media contacted with Mn^{2+} salt.

3.2.3. Toxicity of ZnS:Mn (10%) NPs

When nanoparticles are doped with metal transition cations such as manganese, their toxicity and interactions with living organisms can be different from the undoped nanoparticles. So finally, we evaluated the toxicity of ZnS:Mn (10%) NPs. (All the results describing the toxicity of ZnS:Mn (0.5%), ZnS:Mn (2.0%) and ZnS:Mn (4.0%) are shown in Figures S4-S9).

In Figure 11, we observe that the viability of the algae decreased immediately after the introduction of a content of 100 mg L^{-1} of ZnS:Mn (10%) NPs, and this, in the three aqueous media: it was close to 50% in BG11 and SRW, and close to 20% in SSW. For a concentration of 50 mg L^{-1} of NPs, the viability in BG11 and SSW decreased slightly during the first three days of testing, then gradually increased to the normal value [49]. For a concentration of 20 mg L^{-1}, the viability also decreased, even in SSW from 24h to 72h. We can therefore conclude that a concentration of 100 mg L^{-1} of ZnS:Mn (10%) NPs exhibited strong toxicity towards Chlorella vulgaris and threaten its survival; a lower concentration of these NPs was also toxic to Chlorella vulgaris in SSW. However, if viability

decreased, photosynthetic activity did not decrease (Figure 12), probably through a protective mechanism of carotenoids, a type of non-enzymatic antioxidants, which may act as singlet oxygen quenchers, thus protecting the machinery photosynthetic [50].

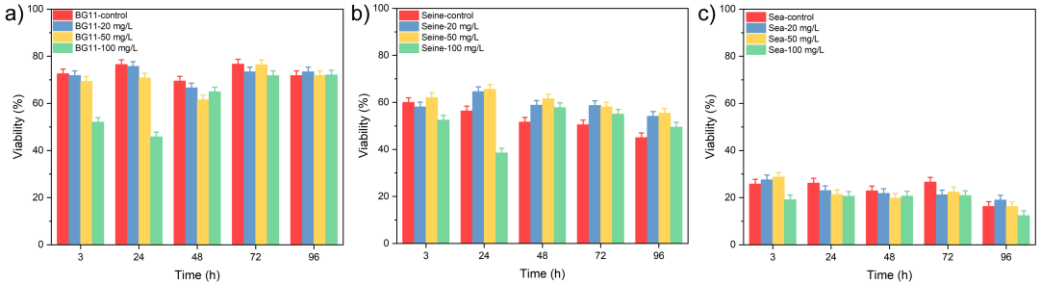

Figure 11. Viability tests of Chlorella vulgaris in a) BG11, b) SRW, c) SSW culture media contacted with ZnS: Mn (10%) NPs.

The influence of NPs on the mitochondrial activity of algae cells was measured through the intracellular ATP content (Figure 12). In BG11, the ATP content decreased after 24 h of exposure, compared to the control group. It is even more affected by a concentration of 50 mg L^{-1}, 72 h later. While mitochondrial activity decreased significantly after 3 h of exposure in SRW and especially in SSW, the toxic effect on mitochondria continued for a long time. The decrease in the ATP content means the decrease in mitochondrial activity, which means that the ZnS:Mn NPs (10%) caused the disruption of the algae's energy metabolism. The SOD activity (Figure 12) increased slightly in BG11, 48 h later, especially in the presence of a concentration of 100 mg $L^{-1}$of NPs. Moreover, SOD activity increased significantly in SRW, 24 h later, while in SSW, SOD activity increased significantly from the very beginning of the test until the last day. Therefore, we can assume that NPs induced the production of ROS, especially in SRW and SSW, which affected the activity of mitochondria, leading to a certain reduction in ATP production, which in turn affected photosynthetic activity and cell viability.

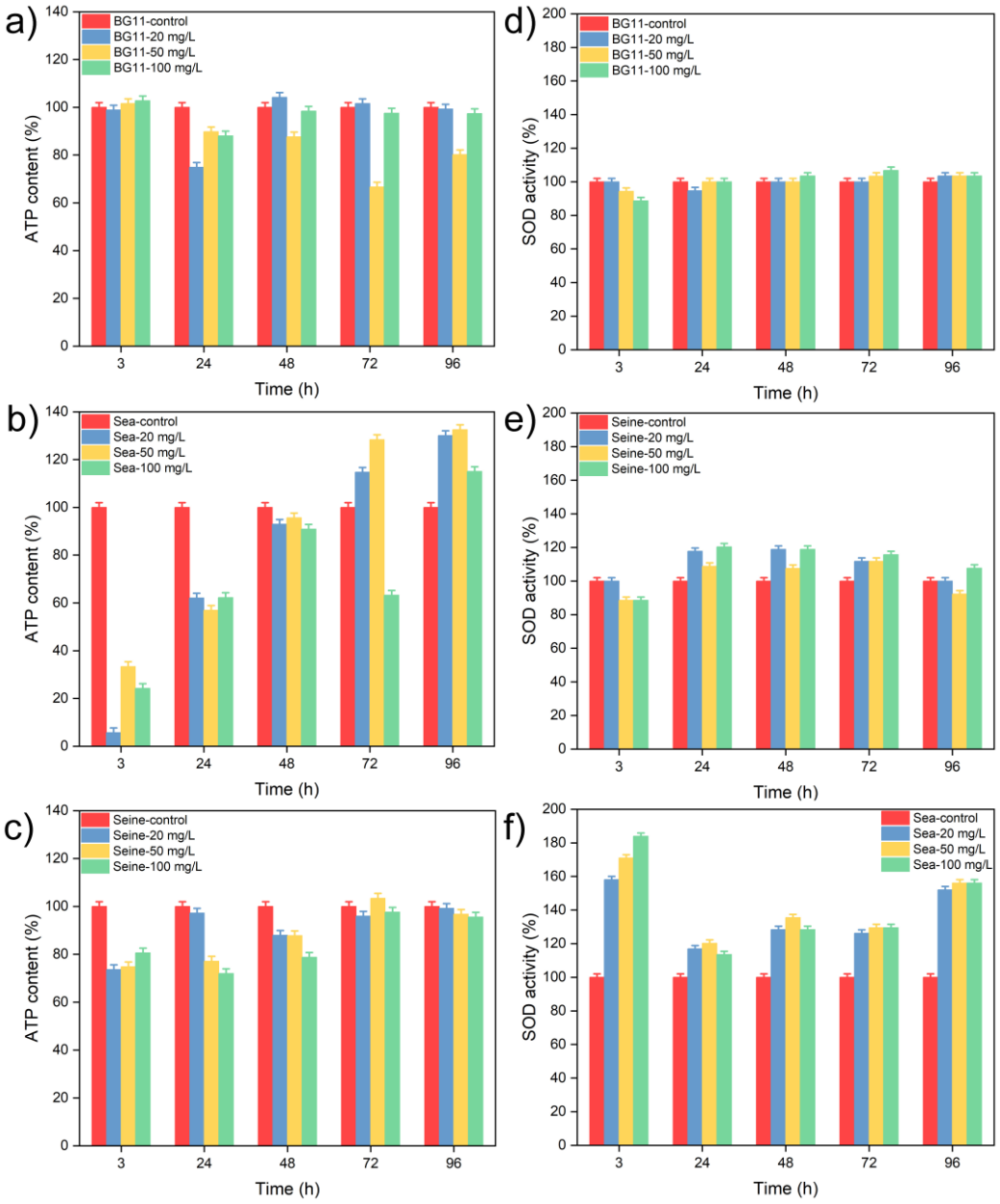

Figure 12. ATP (a-c) and SOD (d-f) tests of Chlorella vulgaris in different culture media contacted with ZnS: Mn (10%) NPs.

Thin-section TEM images of Chlorella vulgaris in the presence or absence of ZnS:Mn (10%) NPs are shown in Figure 13. In the absence of NPs, one can see the integral cell wall and the clear cytoplasm of the algae, whatever the aqueous medium. On the other hand, in the presence of ZnS:Mn (10%) NPs, the cell wall and/or the cytoplasm were damaged. In BG11, we clearly see the dark, circled, spherical aggregate NPs on the cell wall; furthermore, the cytoplasm and the cell wall are clearly separated. In SRW, part of the small-sized NPs also appeared in the cytoplasm, and the cell wall was broken down. Moreover, we can clearly see the number of aggregated NPs inside the algae cell; the cytoplasm has disappeared, and many NPs (circled in the image) were outside the algae cell.

Therefore, we can conclude that the algae cell can internalize ZnS:Mn (10%) NPs by endocytosis, which will destroy the cytoplasm and cell wall of the algae cell and induce lethal danger.

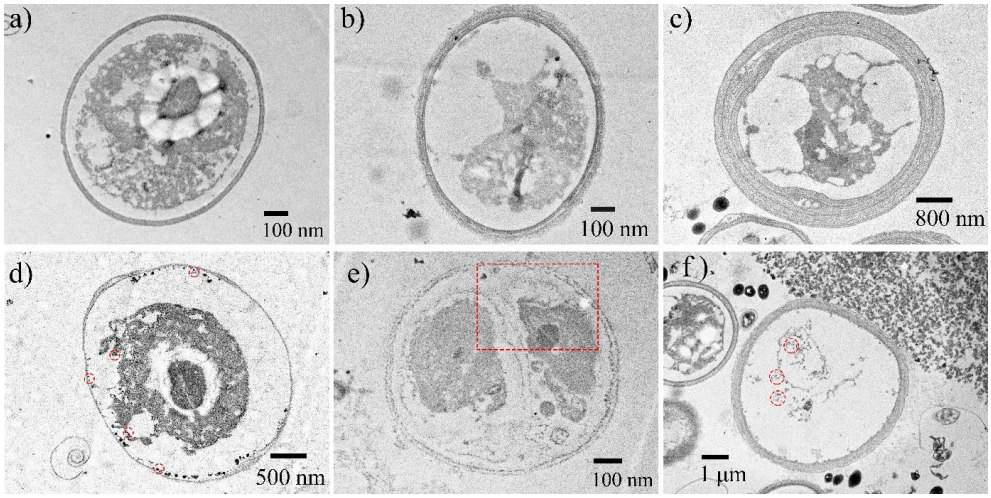

Figure 13. TEM images of Chlorella vulgaris thin sections in different media, (a, d) in BG11, (b, e) in SRW, (c, f) in SSW. (d, e, f) showed the Chlorella vulgaris thin sections after exposure to 100 mg L^{-1} of ZnS:Mn (10%) NPs.

4. Discussion

In this paper, we described the synthesis of ZnS and ZnS:Mn NPs containing different concentrations of Mn^{2+} (from 0.5% to 10%). All the particles synthesized present the same diameter. However, at pH values between 6 and 8, they tend to aggregate to a greater or lesser extent depending on the aqueous medium in which they were dispersed: DLS analyses show that they are much more dispersed in Seine River water and seawater than in fresh water. On the other hand, zeta potential measurements show greater stability in fresh water and Seine River water than in seawater. But in all cases, they are negatively charged and *a priori* difficult to internalize.

Focusing on particles containing 10% Mn^{2+}, ICP-AES shows that almost all Mn^{2+} ions dissolve in Seine River water and seawater, while Zn^{2+} ions dissolve more strongly in fresh and Seine River water.

Toxicity tests showed that ZnS nanoparticles are not toxic to Chlorella Vulgaris in any type of water. Based on the color of the solutions, Mn^{2+} ions appear toxic at concentrations of 100 mg L^{-1}, but viability tests show slighter toxicity in Seine River water. In seawater, however, the toxicity is much higher. Similarly, ZnS:Mn NPs show high toxicity at concentrations of the order of 100 mg L^{-1}. Some of the dissolved ions (probably Zn^{2+} ions) could even serve as nutrients in Seine water.

There's a sudden drop in ATP content in seawater, far greater than in fresh water and Seine River water. This corresponds to a decrease in mitochondrial activity, which means that the ZnS:Mn (10%) NPs cause the disruption of the algae's energy metabolism. However, it increases a little later, still in seawater, which means that algae are adapting to the medium and can produce ATP again.

SOD content is constant in fresh water. It increases slightly in seawater and remains constant, while it increases more rapidly in Seine River before decreasing. NPs induced the production of ROS, which affected the activity of mitochondria, leading to a certain reduction in ATP production, which in turn affected photosynthetic activity and cell viability!

Therefore, ZnS:Mn NPs induce an antioxidant defense system in the algal cell, which is not always able to cope with these attacks. Degradation of subcellular organelles observed on TEM images and oxidative stress are the main consequences of NP toxicity. Various factors can be attributed to this toxicity: the size of the aggregates, their compo-

sition, and their stability in terms of ion dissolution. The study carried out on manganese salt shows that very high concentrations must be reached before Mn^{2+} ions are no longer a nutrient but a poison. And ZnS NPs were found to be non-toxic.

As a result, the *nano* scale can be assumed to be toxic to Chlorella vulgaris, via an oxidative stress mechanism. Moreover, the high surface/volume ratio of NPs allows them (despite the general aggregation that was observed) to spread around the algal cell, thus decreasing the nutrient exchange interface of algal cells, in addition to the internalization of the NPs.

5. Conclusions

The causes of the potential toxicity of manufactured naoparticles are diverse. Added to this is the complexity and diversity of biological environments: two algae cultures may behave differently. Fortunately, Chlorella vulgaris is consistent in its behavior, enabling us to conclude that the toxicity of manganese-doped ZnS nanoparticles does exist, but is lower than that induced by a Mn^{2+} ion concentration of 100 mg L^{-1}, which means that we can confidently envisage the introduction of these particles into miniaturized devices.

Author Contributions: B.D., investigation and methodology; R.M., S.N., Y.S., C.Y., formal analysis; R.B., conceptualization; F.M., S.A., R.B., supervision, B.D., F.M., writing—original draft preparation; R.B. and F.M., project administration.

Funding: ANR (Agence Nationale de la Recherche) and CGI (Commissariat à l'Investissement d'Avenir) are gratefully acknowledged for their financial support of this work through Labex SEAM (Science and Engineering for Advanced Materials and devices), ANR-10-LABX-096 and ANR-18-IDEX-0001. B.D. thanks the China Scholarship Council (CSC no. 201806400081) for the financial support.

Acknowledgments: BD acknowledges Chakib Djediat for his technical support for TEM observations at MNHN and Philippe Decorse for his technical support for XPS analysis. Parts of this work were supported by IPGP multidisciplinary program PARI, and by Paris–IdF region SESAME Grant no. 12015908.

Conflicts of Interest: The authors declare no conflict of interest.

References

1. Nel, A.; Xia, T. Toxic Potential of Materials at the Nanolevel. **2006**, *311*.
2. Brayner, R.; Dahoumane, S.A.; Nguyen, J.N.-L.; Yéprémian, C.; Djediat, C.; Couté, A.; Fiévet, F. Ecotoxicological Studies of CdS Nanoparticles on Photosynthetic Microorganisms. *Journal of Nanoscience and Nanotechnology* **2011**, *11*, 1852–1858, doi:10.1166/jnn.2011.3564.
3. Brayner, R.; Dahoumane, S.A.; Yéprémian, C.; Djediat, C.; Meyer, M.; Couté, A.; Fiévet, F. ZnO Nanoparticles: Synthesis, Characterization, and Ecotoxicological Studies. *Langmuir* **2010**, *26*, 6522–6528, doi:10.1021/la100293s.
4. Mueller, N.C.; Nowack, B. Exposure Modeling of Engineered Nanoparticles in the Environment. *Environ. Sci. Technol.* **2008**, *42*, 4447–4453, doi:10.1021/es7029637.
5. Brayner, R. The Toxicological Impact of Nanoparticles. *Nano Today* **2008**, *3*, 48–55, doi:10.1016/S1748-0132(08)70015-X.
6. Gottschalk, F.; Sonderer, T.; Scholz, R.W.; Nowack, B. Modeled Environmental Concentrations of Engineered Nanomaterials (TiO2, ZnO, Ag, CNT, Fullerenes) for Different Regions. *Environ. Sci. Technol.* **2009**, *43*, 9216–9222, doi:10.1021/es9015553.
7. Nowack, B. The Behavior and Effects of Nanoparticles in the Environment. *Environmental Pollution* **2009**, *157*, 1063–1064, doi:10.1016/j.envpol.2008.12.019.
8. Wang, Y.; Herron, N. Nanometer-Sized Semiconductor Clusters: Materials Synthesis, Quantum Size Effects, and Photophysical Properties. *J. Phys. Chem.* **1991**, *95*, 525–532, doi:10.1021/j100155a009.
9. Longo, A.V.; Notebaert, B.; Gaceur, M.; Patriarche, G.; Sciortino, A.; Cannas, M.; Messina, F.; von Bardeleben, H.J.; Battaglini, N.; Ammar, S. Photo-Activated Phosphorescence of Ultrafine ZnS:Mn Quantum Dots: On the Lattice Strain Contribution. *J. Phys. Chem. C* **2022**, *126*, 1531–1541, doi:10.1021/acs.jpcc.1c09687.
10. Chen, W.; Wang, Z.; Lin, Z.; Lin, L. Absorption and Luminescence of the Surface States in ZnS Nanoparticles. *Journal of Applied Physics* **1997**, *82*, 3111–3115, doi:10.1063/1.366152.
11. Biswas, S.; Kar, S.; Chaudhuri, S. Optical and Magnetic Properties of Manganese-Incorporated Zinc Sulfide Nanorods Synthesized by a Solvothermal Process. *J. Phys. Chem. B* **2005**, *109*, 17526–17530, doi:10.1021/jp053138i.
12. Datta, A.; Biswas, S.; Kar, S.; Chaudhuri, S. Multicolor Luminescence from Transition Metal Ion (Mn^{2+} and Cu^{2+}) Doped ZnS Nanoparticles. *J. Nanosci. Nanotech.* **2007**, *7*, 3670–3676, doi:10.1166/jnn.2007.810.
13. Mishra, P.; Ojha, K.S.; Khare, A. Structural and Optical Study of Copper-Doped Zinc Sulfide Nanoparticles. *J Appl Spectrosc* **2018**, *85*, 743–748, doi:10.1007/s10812-018-0714-5.
14. Manzoor, K.; Vadera, S.R.; Kumar, N.; Kutty, T.R.N. Multicolor Electroluminescent Devices Using Doped ZnS Nanocrystals. *Appl. Phys. Lett.* **2004**, *84*, 284–286, doi:10.1063/1.1639935.
15. Mei, S.; Zhang, G.; Yang, W.; Wei, X.; Zhang, W.; Zhu, J.; Guo, R. A Facile Route for Highly Efficient Color-Tunable Cu-Ga-Se/ZnSe Quantum Dots. *Applied Surface Science* **2018**, *456*, 876–881, doi:10.1016/j.apsusc.2018.06.199.
16. Wei, X.; Mei, S.; Zhang, G.; Su, D.; Xie, F.; Zhang, W.; Guo, R. Enhanced Tunable Dual Emission of Cu:InP/ZnS Quantum Dots Enabled by Introducing Ag Ions. *Applied Surface Science* **2019**, *493*, 605–612, doi:10.1016/j.apsusc.2019.06.059.
17. Chung, J.H.; Ah, C.S.; Jang, D.-J. Formation and Distinctive Decay Times of Surface- and Lattice-Bound Mn^{2+} Impurity Luminescence in ZnS Nanoparticles. *J. Phys. Chem. B* **2001**, *105*, 4128–4132, doi:10.1021/jp002692j.

18. Xu, S.J.; Chua, S.J.; Liu, B.; Gan, L.M.; Chew, C.H.; Xu, G.Q. Luminescence Characteristics of Impurities-Activated ZnS Nanocrystals Prepared in Microemulsion with Hydrothermal Treatment. *Appl. Phys. Lett.* **1998**, *73*, 478–480, doi:10.1063/1.121906.
19. Rocha, A.D.; Sivry, Y.; Gelabert, A.; Beji, Z.; Benedetti, M.F.; Menguy, N.; Brayner, R. The Fate of Polyol-Made ZnO and CdS Nanoparticles in Seine River Water (Paris, France). *j nanosci nanotechnol* **2015**, *15*, 3900–3908, doi:10.1166/jnn.2015.9276.
20. Planchon, M.; Jittawuttipoka, T.; Cassier-Chauvat, C.; Guyot, F.; Gelabert, A.; Benedetti, Marc.F.; Chauvat, F.; Spalla, O. Exopolysaccharides Protect Synechocystis against the Deleterious Effects of Titanium Dioxide Nanoparticles in Natural and Artificial Waters. *Journal of Colloid and Interface Science* **2013**, *405*, 35–43, doi:10.1016/j.jcis.2013.05.061.
21. Planchon, M.; Léger, T.; Spalla, O.; Huber, G.; Ferrari, R. Metabolomic and Proteomic Investigations of Impacts of Titanium Dioxide Nanoparticles on Escherichia Coli. *PLoS ONE* **2017**, *12*, e0178437, doi:10.1371/journal.pone.0178437.
22. Sivry, Y.; Gelabert, A.; Cordier, L.; Ferrari, R.; Lazar, H.; Juillot, F.; Menguy, N.; Benedetti, M.F. Behavior and Fate of Industrial Zinc Oxide Nanoparticles in a Carbonate-Rich River Water. *Chemosphere* **2014**, *95*, 519–526, doi:10.1016/j.chemosphere.2013.09.110.
23. Kube, M.; Mohseni, A.; Fan, L.; Roddick, F. Impact of Alginate Selection for Wastewater Treatment by Immobilised Chlorella Vulgaris. *Chemical Engineering Journal* **2019**, *358*, 1601–1609, doi:10.1016/j.cej.2018.10.065.
24. Gao, F.; Cui, W.; Xu, J.-P.; Li, C.; Jin, W.-H.; Yang, H.-L. Lipid Accumulation Properties of Chlorella Vulgaris and Scenedesmus Obliquus in Membrane Photobioreactor (MPBR) Fed with Secondary Effluent from Municipal Wastewater Treatment Plant. *Renewable Energy* **2019**, *136*, 671–676, doi:10.1016/j.renene.2019.01.038.
25. Dziwulska, U.; Bajguz, A.; Godlewska-Żyłkiewicz, B. The Use of Algae *Chlorella Vulgaris* Immobilized on Cellex-T Support for Separation/Preconcentration of Trace Amounts of Platinum and Palladium before GFAAS Determination. *Analytical Letters* **2004**, *37*, 2189–2203, doi:10.1081/AL-200026696.
26. Kaplan, D.; Heimer, Y.M.; Abeliovich, A.; Goldsbrough, P.B. Cadmium Toxicity and Resistance in Chlorella Sp. *Plant Science* **1995**, *109*, 129–137, doi:10.1016/0168-9452(95)04165-Q.
27. Kim, J.; Lingaraju, B.P.; Rheaume, R.; Lee, J.-Y.; Siddiqui, K.F. Removal of Ammonia from Wastewater Effluent by Chlorella Vulgaris. *Tinshhua Sci. Technol.* **2010**, *15*, 391–396, doi:10.1016/S1007-0214(10)70078-X.
28. Lutterotti, L. MAUD Tutorial - Instrumental Broadening Determination.
29. Murugadoss, G. Synthesis and Photoluminescence Properties of Zinc Sulfide Nanoparticles Doped with Copper Using Effective Surfactants. *Particuology* **2013**, *11*, 566–573, doi:10.1016/j.partic.2012.11.003.
30. Sakthivel, P.; Prasanna Venkatesan, G.K.D.; Subramaniam, K.; Muthukrishnan, P. Structural, Optical, Photoluminescence and Electrochemical Behaviours of Mg, Mn Dual-Doped ZnS Quantum Dots. *J Mater Sci: Mater Electron* **2019**, *30*, 11984–11993, doi:10.1007/s10854-019-01551-2.
31. Chaguetmi, S.; Chaperman, L.; Nowak, S.; Schaming, D.; Lau-Truong, S.; Decorse, P.; Beaunier, P.; Costentin, C.; Mammeri, F.; Achour, S.; et al. Photoelectrochemical Properties of ZnS- and CdS-TiO_2 Nanostructured Photocatalysts: Aqueous Sulfidation as a Smart Route to Improve Catalyst Stability. *Journal of Photochemistry and Photobiology A: Chemistry* **2018**, *356*, 489–501, doi:10.1016/j.jphotochem.2018.01.038.
32. Zhu, Y.-P.; Li, J.; Ma, T.-Y.; Liu, Y.-P.; Du, G.; Yuan, Z.-Y. Sonochemistry-Assisted Synthesis and Optical Properties of Mesoporous ZnS Nanomaterials. *Journal of Materials Chemistry A* **2014**, *2*, 1093–1101, doi:10.1039/C3TA13636A.

33. Do, Y.R.; Park, D.H.; Yang, H.G.; Park, W.; Wagner, B.K.; Yasuda, K.; Summers, C.J. Uniform Nanoscale SiO_2 Encapsulation of ZnS Phosphors for Improved Aging Properties under Low Voltage Electron Beam Excitation. *J. Electrochem. Soc.* **2001**, *148*, G548–G551, doi:10.1149/1.1397775.
34. Labiadh, H.; Sellami, B.; Khazri, A.; Saidani, W.; Khemais, S. Optical Properties and Toxicity of Undoped and Mn-Doped ZnS Semiconductor Nanoparticles Synthesized through the Aqueous Route. *Optical Materials* **2017**, *64*, 179–186, doi:10.1016/j.optmat.2016.12.011.
35. Zhou, D.-J.; Xie, X.-Y.; Zhang, Y.; Guo, D.-Y.; Zhou, Y.-J.; Xie, J.-F. Facile Synthesis of ZnS Nanorods in PEG and Their Spectral Performance. *Mater. Res. Express* **2016**, *3*, 105023, doi:10.1088/2053-1591/3/10/105023.
36. Chaguetmi, S.; Mammeri, F.; Nowak, S.; Decorse, P.; Lecoq, H.; Gaceur, M.; Naceur, J.B.; Achour, S.; Chtourou, R.; Ammar, S. Photocatalytic Activity of TiO_2 Nanofibers Sensitized with ZnS Quantum Dots. *RSC Advances* **2013**, *3*, 2572–2580, doi:10.1039/C2RA21684A.
37. Liu, W.; Chen, S. An Investigation of the Tribological Behaviour of Surface-Modified ZnS Nanoparticles in Liquid Paraffin. *Wear* **2000**, *238*, 120–124, doi:10.1016/S0043-1648(99)00344-0.
38. Geszke, M.; Murias, M.; Balan, L.; Medjahdi, G.; Korczynski, J.; Moritz, M.; Lulek, J.; Schneider, R. Folic Acid-Conjugated Core/Shell ZnS:Mn/ZnS Quantum Dots as Targeted Probes for Two Photon Fluorescence Imaging of Cancer Cells. *Acta Biomaterialia* **2011**, *7*, 1327–1338, doi:10.1016/j.actbio.2010.10.012.
39. Kolmykov, O.; Coulon, J.; Lalevée, J.; Alem, H.; Medjahdi, G.; Schneider, R. Aqueous Synthesis of Highly Luminescent Glutathione-Capped Mn^{2+}-Doped ZnS Quantum Dots. *Materials Science and Engineering: C* **2014**, *44*, 17–23, doi:10.1016/j.msec.2014.07.064.
40. Bwatanglang, I.B.; Mohammad, F.; Yusof, N.A.; Abdullah, J.; Hussein, M.Z.; Alitheen, N.B.; Abu, N. Folic Acid Targeted Mn:ZnS Quantum Dots for Theranostic Applications of Cancer Cell Imaging and Therapy. *Int J Nanomedicine* **2016**, *11*, 413–428, doi:10.2147/IJN.S90198.
41. Sumboja, A.; Ge, X.; Goh, F.W.T.; Li, B.; Geng, D.; Hor, T.S.A.; Zong, Y.; Liu, Z. Manganese Oxide Catalyst Grown on Carbon Paper as an Air Cathode for High-Performance Rechargeable Zinc–Air Batteries. *ChemPlusChem* **2015**, *80*, 1341–1346, doi:10.1002/cplu.201500183.
42. Munk, M.; Brandão, H.M.; Nowak, S.; Mouton, L.; Gern, J.C.; Guimaraes, A.S.; Yéprémian, C.; Couté, A.; Raposo, N.R.B.; Marconcini, J.M.; et al. Direct and Indirect Toxic Effects of Cotton-Derived Cellulose Nanofibres on Filamentous Green Algae. *Ecotoxicology and Environmental Safety* **2015**, *122*, 399–405, doi:10.1016/j.ecoenv.2015.09.001.
43. Ding, H.; Ma, Y. Controlling Cellular Uptake of Nanoparticles with PH-Sensitive Polymers. *Sci Rep* **2013**, *3*, 2804, doi:10.1038/srep02804.
44. Polonini, H.C.; Brandão, H.M.; Raposo, N.R.B.; Brandão, M.A.F.; Mouton, L.; Couté, A.; Yéprémian, C.; Sivry, Y.; Brayner, R. Size-Dependent Ecotoxicity of Barium Titanate Particles: The Case of Chlorella Vulgaris Green Algae. *Ecotoxicology* **2015**, *24*, 938–948, doi:10.1007/s10646-015-1436-6.
45. Haniu, H.; Saito, N.; Matsuda, Y.; Tsukahara, T.; Maruyama, K.; Usui, Y.; Aoki, K.; Takanashi, S.; Kobayashi, S.; Nomura, H.; et al. Culture Medium Type Affects Endocytosis of Multi-Walled Carbon Nanotubes in BEAS-2B Cells and Subsequent Biological Response. *Toxicology in Vitro* **2013**, *27*, 1679–1685, doi:10.1016/j.tiv.2013.04.012.
46. Gaceur, M.; Giraud, M.; Hemadi, M.; Nowak, S.; Menguy, N.; Quisefit, J.P.; David, K.; Jahanbin, T.; Benderbous, S.; Boissière, M.; et al. Polyol-Synthesized $Zn_{0.9}Mn_{0.1}S$ Nanoparticles as Potential Luminescent and Magnetic Bimodal Imaging Probes: Synthesis, Characterization, and Toxicity Study. *Journal of Nanoparticle Research* **2012**, *14*, doi:10.1007/s11051-012-0932-3.

47. Jahanbin, T.; Gaceur, M.; Gros-Dagnac, H.; Benderbous, S.; Merah, S.A. High Potential of Mn-Doped ZnS Nanoparticles with Different Dopant Concentrations as Novel MRI Contrast Agents: Synthesis and in Vitro Relaxivity Studies. *J Nanopart Res* **2015**, *17*, 258, doi:10.1007/s11051-015-3038-x.
48. Planchon, M.; Ferrari, R.; Guyot, F.; Gélabert, A.; Menguy, N.; Chanéac, C.; Thill, A.; Benedetti, M.F.; Spalla, O. Interaction between Escherichia Coli and TiO_2 Nanoparticles in Natural and Artificial Waters. *Colloids and Surfaces B: Biointerfaces* **2013**, *102*, 158–164, doi:10.1016/j.colsurfb.2012.08.034.
49. da Rocha, A.; Menguy, N.; Yéprémian, C.; Couté, A.; Brayner, R. Ecotoxicological Studies of ZnO and CdS Nanoparticles on Chlorella Vulgaris Photosynthetic Microorganism in Seine River Water. *Nanomaterials (Basel)* **2020**, *10*, doi:10.3390/nano10020227.
50. Furger, C. Live Cell Assays for the Assessment of Antioxidant Activities of Plant Extracts. *Antioxidants* **2021**, *10*, 944, doi:10.3390/antiox10060944.